1640 *Chem. Mater.* **2010,** *22,* 1640–1646
DOI:10.1021/cm902718r

CHEMISTRY OF MATERIALS
Article

Synthesis and Structural Studies of the Transition-Metal-Doped Rh Perovskites $LaMn_{0.5}Rh_{0.5}O_3$ and $LaCu_{0.5}Rh_{0.5}O_3$

Jimmy Ting,[†] Brendan J. Kennedy,*[,†] Zhaoming Zhang,[‡] Maxim Avdeev,[§] Bernt Johannessen,[||] and Ling-Yun Jang[#]

[†]*School of Chemistry, The University of Sydney, Sydney NSW 2006, Australia,* [‡]*Institute of Materials Engineering, and* [§]*Bragg Institute, Australian Nuclear Science and Technology Organisation, Private Mail Bag 1, Menai NSW 2234, Australia,* [||]*Australian Synchrotron, 800 Blackburn Road, Clayton, Victoria 3168, Australia, and* [#]*Research Division, National Synchrotron Radiation Research Center, Hsinchu 300, Taiwan*

Received September 1, 2009. Revised Manuscript Received December 17, 2009

The two orthorhombic perovskites $LaMn_{0.5}Rh_{0.5}O_3$ and $LaCu_{0.5}Rh_{0.5}O_3$ have been characterized using X-ray absorption near edge structure (XANES) measurements and powder synchrotron X-ray and neutron diffraction. The Mn and Rh in $LaMn_{0.5}Rh_{0.5}O_3$ are essentially trivalent and disordered onto the same crystallographic site. The absence of an appreciable Jahn−Teller (JT) distortion of the BO_6 octahedra is a consequence of this disorder and large magnitude of the octahedral tilting. XANES measurements show that the Rh in $LaCu_{0.5}Rh_{0.5}O_3$ has a valence state of around +3.5 as a consequence of extensive charge delocalization between the Cu and Rh cations, that are also disordered onto a single site. These two effects combine to further reduce the distortion of the octahedra in $LaCu_{0.5}Rh_{0.5}O_3$ relative to that of $LaMn_{0.5}Rh_{0.5}O_3$.

Introduction

The perovskite structure is one of the most frequently encountered structural types in solid-state chemistry. Perovskite oxides have the general formula ABO_3 where the larger *A*-type cations are surrounded by 12 oxygen anions in a cuboctahedral coordination and the smaller *B*-type cations are surrounded by six oxygen anions in octahedral arrangement. In the ideal case, the perovskites are cubic in space group $Pm\bar{3}m$, although in many cases cooperative tilting of the corner sharing BO_6 octahedra occurs in response to a size mismatch between the *A*- and *B*-type cations. The family of perovskites can be extended by chemical substitution at either cation site, and in recent years there has been considerable interest in oxides that contain two cations in the octahedral site, $AB_{1-x}B'_xO_3$. In the case where $x = 0.5$, cation ordering to form a three-dimensional network of alternating BO_6 and $B'O_6$ octahedra is often observed, although the *B* and *B*′ cations can also adopt a disordered arrangement if their size and oxidation state are similar. Much of the recent interest in these oxides has been driven by their unusual magnetic properties, especially in those oxides that contain both a first row and a heavier, 4d or 5d, transition metal.

Despite the tendency for perovskites to exhibit symmetry lowering by tilting, the bond distances within the octahedra tend to remain relatively symmetric in the absence of electronic effects. The most commonly encountered electronic distortions are the polar displacements in oxides where the *B*-site cation has a d^0 electronic configuration such as in $BaTiO_3$ or $PbTi_{1-x}Zr_xO_3$ or Jahn−Teller type distortions where the *B*-site cation has an appropriate electronic configuration, such as Mn^{3+} (d^4) or Cu^{2+} (d^9). Anisotropic occupancy of the e_g orbitals in Mn^{3+}-containing perovskites can result in a long-range orbital ordering, leading to an array of complex and often fascinating phenomena. Incorporating a heavier transition metal, such as Ru[1,2] or Ir[3] into a manganese perovskite has been studied as a means to tune the properties of such oxides. Studies of mixed Mn−Ru perovskites such as $SrMn_{0.5}Ru_{0.5}O_3$ have demonstrated a complex interplay between the orbital ordering, octahedral tilting, and electron transfer between the Mn and Ru cations.[4−6]

The aim of the present paper is to describe the structure and valence states of two mixed-metal perovskites $LaMn_{0.5}Rh_{0.5}O_3$ and $LaCu_{0.5}Rh_{0.5}O_3$. Although the structure of $LaMn_{0.5}Rh_{0.5}O_3$ has been reported previously,[7,8] only a conventional laboratory X-ray source was used. In the present study, we have employed both synchrotron X-ray (more sensitive to detect any cation

*Corresponding author.

(1) Kolesnik, S.; Dabrowski, B.; Chmaissem, O. *Phys. Rev. B* **2008**, *78*, 214425.
(2) Mizusaki, S.; Taniguchi, T.; Okada, N.; Nagata, Y.; Hiraoka, N.; Itou, M.; Sakurai, Y.; Noro, Y.; Ozawa, T. C.; Samata, H. *J. Phys.: Condens. Matter* **2009**, *21*, 276003.
(3) Mizusaki, S.; Sato, J.; Taniguchi, T.; Nagata, Y.; Lai, S. H.; Lan, M. D.; Ozawa, T. C.; Noro, Y.; Samata, H. *J. Phys.: Condens. Matter* **2008**, *20*, 235242.
(4) Sahu, R. K.; Hu, Z.; Rao, M. L.; Manoharan, S. S.; Schmidt, T.; Richter, B.; Knupfer, M.; Golden, M.; Fink, J.; Schneider, C. M. *Phys. Rev. B* **2002**, *66*, 144415.
(5) Kennedy, B. J.; Zhou, Q. *Solid State Commun.* **2008**, *147*, 208–211.
(6) Lufaso, M. W.; Woodward, P. M.; Goldberger, J. *J. Solid State Chem.* **2004**, *177*, 1651–1659.
(7) Schinzer, C. *J. Phys. Chem. Solids* **2000**, *61*, 1543–1551.
(8) Haque, M. T.; Kamegashira, N. *J. Alloys Compd.* **2005**, *395*, 220–226.

Published on Web 02/12/2010

ordering) and neutron powder diffraction (for the determination of precise bond distances) to study these two compounds. Furthermore, the oxidation states of the *B*-site cations in these two samples were determined, for the first time, using XANES. These two oxides are found to be isostructural without cation ordering, but with differing formal oxidation states of the *B*-site cations.

Experimental Section

Polycrystalline samples of $LaRhO_3$, $LaMn_{0.5}Rh_{0.5}O_3$, $LaCu_{0.5}Rh_{0.5}O_3$, and La_2MgRhO_6 (double formula is used to indicate Mg/Rh ordering) were prepared by solid-state reaction from stoichiometric mixtures of high-purity La_2O_3, Rh metal and the appropriate metal oxide (Mn_2O_3, CuO, and MgO). After mixing, the powders were placed in alumina crucibles and calcined at 950 °C overnight before being heated at 1300 °C for 6 days with periodic regrinding of the mixture. The samples were heated under an oxygen atmosphere to promote oxidation of the Rh metal. The reactions were continued until powder X-ray diffraction patterns, collected using a Shimadzu D6000 diffractometer, no longer changed.

X-ray diffraction data were collected on the high resolution Debye−Scherrer diffractometer at the Australian National Beamline Facility (ANBF), Beamline 20B at the Photon Factory, Tsukuba, Japan.[9] The samples were housed in 0.3 mm diameter glass capillaries that were rotated during the measurements. The data were recorded at room temperature over the angular range $5° < 2\theta < 85°$, step size 0.01° using X-rays of wavelength 0.80286 Å with two Fuji Image plates being used as detector. Each image plate is 20 × 40 cm and covers 40° in 2θ. The wavelength was calibrated using Si 640c as a standard. Neutron powder diffraction data were measured using the high resolution powder diffractometer Echidna[10] at ANSTO's OPAL facility at Lucas Heights, Australia using neutrons of wavelength 1.538 Å. For these measurements the samples were contained in a cylindrical vanadium can. The structures were refined using the program RIETICA,[11] where the background was estimated by interpolating between up to 40 selected points.

Rh $L_{3,2}$-edge and Mn K-edge X-ray absorption spectra were recorded, from powder samples dispersed on Kapton tape, in fluorescence mode on beamline BL-16A1 at the National Synchrotron Radiation Research Center (NSRRC) in Hsinchu, Taiwan using a Lytle detector.[12] Energy steps as small as 0.2 eV were employed near the absorption edges with a counting time of 2 s per step. The spectra were normalized to the incident photon current. The energy scale of the Rh $L_{3,2}$- and Mn K-edge spectra was calibrated using the L_2-edge of a Mo foil and K-edge of a Mn foil respectively. $LaRhO_3$ and La_2MgRhO_6 were used as the Rh^{3+} and Rh^{4+} standards. Data analysis was carried out using the software package EXAFSPAK.[13] First the BACKSUB program was used for background subtraction and normalization, followed by least-squares refinement (DATFIT).

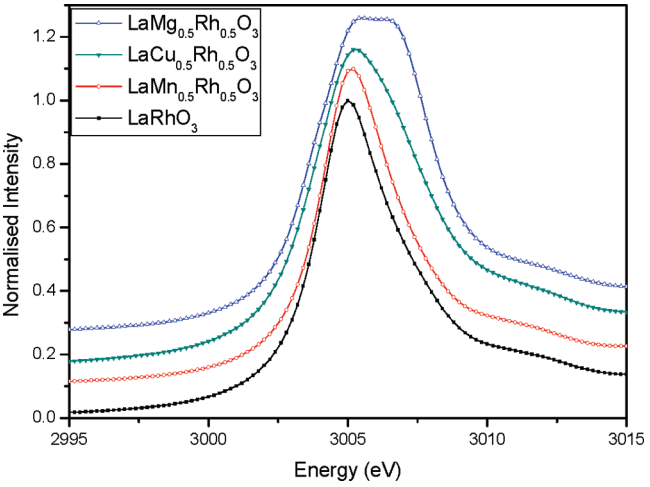

Figure 1. Normalized Rh L_3-edge XANES spectra for members in the series $LaB_{0.5}Rh_{0.5}O_3$, and Rh^{3+} ($LaRhO_3$) and Rh^{4+} (La_2MgRhO_6) standards. The data have been offset vertically for clarity.

Cu K-edge X-ray absorption spectra were recorded in transmission mode on beamline 12ID at the Australian Synchrotron in Melbourne, Australia using a set of flow-through ion chambers filled with N_2. Energy steps of 0.25 eV were employed near the edge while counting for 1 s per step. The energy scale was calibrated by simultaneously measuring a Cu foil placed between two downstream ion chambers.

The magnetic measurements were carried out using a SQUID magnetometer (Quantum Design, MPMS-5S). The temperature dependence of the magnetic susceptibilities was measured under both zero-field-cooled (ZFC) and field-cooled (FC) conditions in an applied field of 0.5 T over the temperature range 5−300 K. The temperature dependence of the resistivity was measured using a DC four-probe technique with the same measurement system (PPMS model). The sintered samples were cut into pieces of approximately 3 × 5 mm. Four contacts were painted onto the samples using carbon paste.

Results and Discussion

Neither the structure nor the oxidation state distribution in $LaCu_{0.5}Rh_{0.5}O_3$ has been established previously. Although two earlier studies of $LaMn_{0.5}Rh_{0.5}O_3$[7,8] both reported the structure to be orthorhombic without any Mn−Rh long-range ordering, there was disagreement over the oxidation states of *B*-site cations in this sample. Schnizer[7] assumed that the Mn and Rh were present as Mn^{2+} and Rh^{4+} based on the fact that no strong JT distortion (expected from Mn^{3+} ions) was observed in the structure. Using magnetic susceptibility measurements Haque et al.[8,14] suggested the oxidation state distribution was actually Mn^{3+}−Rh^{3+} rather than Mn^{2+}−Rh^{4+}. Recent magnetic studies by Sheets et al.[15] on $LaMn_{0.5}Rh_{0.5}O_3$ thin films were interpreted assuming a Mn^{2+}−Rh^{4+} distribution, although these authors acknowledged that the observed ferromagnetism could also arise from disorder of Mn^{3+} and Rh^{3+} cations.

(9) Sabine, T. M.; Kennedy, B. J.; Garrett, R. F.; Foran, G. J.; Cookson, D. J. *J. Appl. Crystallogr.* **1995**, *28*, 513–517.
(10) Liss, K.-D.; Hunter, B.; Hagen, M.; Noakes, T.; Kennedy, S. *Physica B* **2006**, *385−386*, 1010–1012.
(11) Hunter, B.A.; , Howard, C.J. *Rietica: A Computer Program for Rietveld Analysis of X-Ray and Neutron Powder Diffraction Patterns*; Lucas Heights Research Laboratories: Sydney, 1998.
(12) Dann, T. E.; Chung, S. C.; Huang, L. J.; Juang, J. M.; Chen, C. I.; Tsang, K. L. *J. Synchrotron Radiat.* **1998**, *5*, 664–666.
(13) George, G. N.; , Pickering, I. J. *EAXFSPAK: A Suite of Computer Programs for Analysis of X-ray Absorption Spectra*; Stanford Synchrotron Radiation Laboratory: Menlo Park, CA, 2000.
(14) Haque, M. T.; Satoh, H.; Kamegashira, N. *J. Alloys Compd.* **2005**, *390*, 115–121.
(15) Sheets, W. C.; Smith, A. E.; Subramanian, M. A.; Prellier, W. *J. Appl. Phys.* **2009**, *105*, 023915.

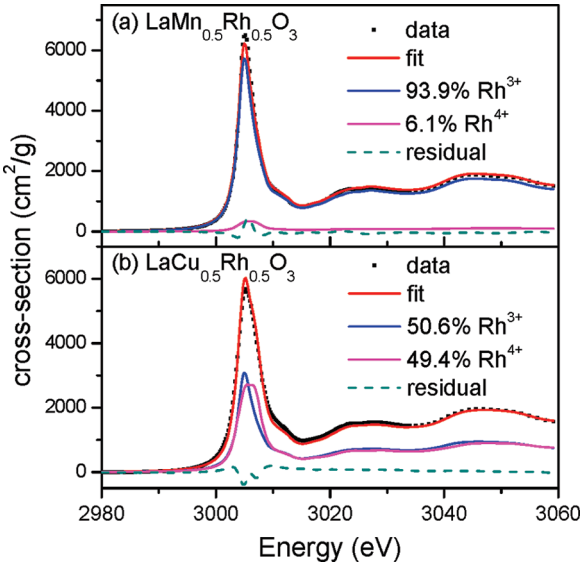

Figure 2. Rh L_3-edge XANES spectra of (a) $LaMn_{0.5}Rh_{0.5}O_3$ and (b) $LaCu_{0.5}Rh_{0.5}O_3$, as well as the corresponding fit and the individual Rh^{3+} ($LaRhO_3$) and Rh^{4+} (La_2MgRhO_6) components.

To establish the valence states of the constituent cations XANES data were collected. The normalized Rh L_3 XANES spectra of $LaCu_{0.5}Rh_{0.5}O_3$, $LaMn_{0.5}Rh_{0.5}O_3$, and Rh^{3+} ($LaRhO_3$) and Rh^{4+} (La_2MgRhO_6) standards are presented in Figure 1. The Rh L-edge absorption spectra originate from dipole allowed transitions of the Rh 2p core electrons into the unoccupied Rh 4d states in the conduction band, which consist of the t_{2g} and e_g orbitals in octahedral symmetry. The splitting of the L-edge into L_3 and L_2 edges arises from spin−orbit coupling (the Rh L_2-edge spectra were also obtained, and show similar features to those of the L_3-edge). As shown in Figure 1, the L_3-edge spectrum of the Rh^{4+} ($4d^5$) oxide La_2MgRhO_6 is characterized by a poorly resolved doublet near 3005.4 and 3006.5 eV, reflecting transitions into the t_{2g} and e_g states, respectively. Conversely, the L_3 spectrum of the Rh^{3+} ($4d^6$) standard $LaRhO_3$ presents a single peak near 3005.0 eV, due to completely filled t_{2g} orbitals (so that only transitions from the $2p_{3/2}$ core levels to the e_g states are possible).[16]

As shown in Figure 1, the Rh L_3-edge XANES spectrum of $LaMn_{0.5}Rh_{0.5}O_3$ is very similar to that of $LaRhO_3$, suggesting that the Rh is predominantly trivalent in $LaMn_{0.5}Rh_{0.5}O_3$. This is confirmed by quantitative analysis using a least-squares refinement program (DATFIT) within the EXAFSPAK software package.[13] Namely, the L_3-edge XANES spectrum from $LaMn_{0.5}Rh_{0.5}O_3$ was fitted with a linear combination of the two standards ($LaRhO_3$ and La_2RhMgO_6) over the energy range of 2980−3060 eV (Figure 2a), giving rise to an average Rh oxidation state of 3.06. The Mn K-edge spectrum was also obtained from $LaMn_{0.5}Rh_{0.5}O_3$ (not shown), and similar

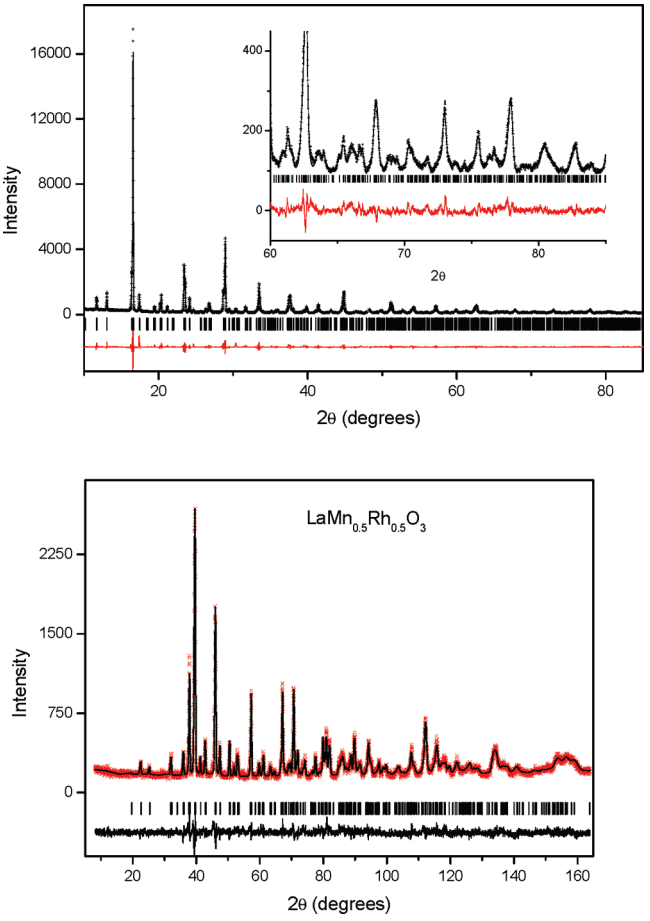

Figure 3. Observed, calculated, and difference synchrotron X-ray (top) and neutron (bottom) diffraction patterns for $LaMn_{0.5}Rh_{0.5}O_3$ refined in the orthorhombic space group *Pbnm*. The inset to the X-ray profile highlights the quality of the data and fit to high angles.

to that of $LaMn^{3+}{}_{0.5}Ga_{0.5}O_3$.[17] Based on both Rh L- and Mn K-edge XANES data we propose the presence of a Mn^{3+}−Rh^{3+} redox distribution in $LaMn_{0.5}Rh_{0.5}O_3$.

The Rh L_3-edge XANES spectrum for $LaCu_{0.5}Rh_{0.5}O_3$ appears intermediate between the two extremes represented by $LaRhO_3$ and La_2MgRhO_6 (Figure 1), suggesting that some degree of electron transfer between the Rh and Cu has occurred. Quantitative analysis of the Rh L_3-edge XANES spectra of $LaCu_{0.5}Rh_{0.5}O_3$ was also undertaken (Figure 2b). The fitting results suggest that the Rh has an average valence of around 3.5. The Cu K-edge spectrum was also examined. However in the absence of suitable Cu^{2+}/Cu^{3+} standards, detailed analysis of the observed Cu K-edge spectrum was not possible, but its appearance is not inconsistent with the partial oxidation of the Cu from 2+ to 3+ in $LaCu_{0.5}Rh_{0.5}O_3$.

The synchrotron X-ray pattern confirmed that $LaMn_{0.5}Rh_{0.5}O_3$ is orthorhombic in space group *Pbnm*, isostructural with $LaRhO_3$[18] and $LaMnO_3$[19], and we find no evidence for long-range ordering of the Mn and Rh cations. Ultimately, the structure was refined using powder neutron diffraction data, the results of which are

(16) Burnus, T.; Hu, Z.; Wu, H.; Cezar, J. C.; Niitaka, S.; Takagi, H.; Chang, C. F.; Brookes, N. B.; Lin, H. J.; Jang, L. Y.; Tanaka, A.; Liang, K. S.; Chen, C. T.; Tjeng, L. H. *Phys. Rev. B* **2008**, *77*, 205111.
(17) Sánchez, M. C.; Subías, G.; García, J.; Blasco, J. *Phys. Rev. B* **2004**, *69*, 184415.
(18) Macquart, R. B.; Smith, M. D.; zur Loye, H.-C. *Cryst. Growth Des.* **2006**, *6*, 1361–1365.
(19) Rodríguez-Carvajal, J.; Hennion, M.; Moussa, F.; Moudden, A. H.; Pinsard, L.; Revcolevschi, A. *Phys. Rev. B* **1998**, *57*, R3189.

Table 1. Results of the Structural Refinements for $LaMn_{0.5}Rh_{0.5}O_3$ and $LaCu_{0.5}Rh_{0.5}O_3$ Using Neutron Powder Diffraction Data; The *B* Site Cations are at 0 0 0

	$LaMn_{0.5}Rh_{0.5}O_3$	$LaCu_{0.5}Rh_{0.5}O_3$
a (Å)	5.5520(4)	5.5507(3)
b (Å)	5.5966(4)	5.6776(3)
c (Å)	7.8502(6)	7.8306(5)
V (Å^3)	243.94(4)	246.74(4)
La *x*	0.5131(10)	0.5086(8)
La *y*	0.0407(7)	0.0498(4)
La *z*	1/4	1/4
La B_{iso}	0.73(6)	1.07(5)
B/Rh B_{iso} (Å^2)	0.00(3)	1.11(6)
O1 *x*	0.4116(10)	0.4095(9)
O1 *y*	0.4875(11)	0.4829(8)
O1 *z*	1/4	1/4
O1 B_{iso} (Å^2)	0.70(13)	0.96(7)
O2 *x*	0.2845(7)	0.2954(6)
O2 *y*	0.2082(7)	0.2015(5)
O2 *z*	−0.0388(6)	−0.0475(4)
O2 B_{iso} (Å^2)	0.96(9)	1.33(5)
B/Rh−O1 (Å)	2.024(1)	2.023(1)
B/Rh−O2 (Å)	1.986(4)	2.033(3)
B/Rh−O2′ (Å)	2.048(4)	2.073(3)
B/Rh−O (av)	2.019	2.043
R_p (profile) (%)	7.58	7.95
R_{wp} (weighted profile) (%)	8.56	10.08

illustrated in Figure 3 and summarized in Table 1. In these refinements, the displacement parameters of the Mn and Rh were constrained to be equal. Refinement of the oxygen occupancies did not lead to any significant deviations from full occupancy, suggesting that any deviation in oxygen stoichiometry is, at most, small. Very similar refinement results were obtained using the synchrotron X-ray diffraction data. We note that the refinements using the neutron diffraction data resulted in unusually low values for the displacement parameter of the Mn/Rh site; we believe this is a consequence of the opposite scattering lengths of Mn (−0.373 fm) and Rh (0.588 fm). The BO_6 octahedra in $LaMn_{0.5}Rh_{0.5}O_3$ are not regular, rather two of the *B*−O distances are somewhat longer than the other four (2 × 2.048(4), 2 × 2.024(1) and 2 × 1.986(4) Å). The distortion of octahedra can be quantified using the expression $\Delta d = (1/6)\Sigma[(d_n - d)/d]^2$, where *d* is the mean *B*−O distance and d_n the individual Mn(Rh)−O distance;[19] Δd has a value of 1.9×10^{-4} for the $LaMn_{0.5}Rh_{0.5}O_3$ sample, which is roughly 1 order of magnitude lower than that for $LaMnO_3$ (33.1×10^{-4})[19] but 1 order of magnitude higher than that for $LaRhO_3$ (0.25×10^{-4}).[18] Bond valence calculation, performed using the refined *B*−O distances obtained from the neutron diffraction data, resulted in values of 2.98 and 3.25 for Mn and Rh, respectively, in keeping with both the Mn and Rh being trivalent in $LaMn_{0.5}Rh_{0.5}O_3$.

The distortion of the $(Mn/Rh)O_6$ octahedra in $LaMn_{0.5}Rh_{0.5}O_3$ may be explained by analogy with the situation in $LaMnO_3$ where the $d_{3x^2}-r^2$ and $d_{3y^2}-r^2$ orbitals are ordered in an alternate staggered pattern in the *a*-*b* plane.[20] This leads to two long and two short Mn/Rh−O bonds in the *a*−*b* plane with the Mn/Rh−O bonds along the *c*-axis being intermediate between these. Previous studies of $LaMn_{1-x}Ga_xO_3$[17] reported that doping of the Mn site with Ga reduces the orbital ordering, ultimately the six Mn/Ga−O bond distances become approximately equal for $x \approx 0.6$. Although the bond length anisotropy in $LaMn_{0.5}Rh_{0.5}O_3$ is considerably less than that observed in $LaMnO_3$, the pattern of 2 long + 2 short + 2 medium bonds is evident, suggesting that orbital ordering associated with a cooperative JT distortion persists in this oxide. We note that in oxides such as $CaMn_{0.5}Nb_{0.5}O_3$ and $CaMn_{0.5}Sb_{0.5}O_3$ the six Mn/*B*−O bond distances are approximately equal and it has been proposed that tilting of the octahedra inhibits a static JT distortion.[6] The out-of-phase tilt angle (φ) around the [110] axis in $LaMn_{0.5}Rh_{0.5}O_3$ at room temperature, estimated from the refined atomic coordinates, is 13.8° and the in-phase angle (ψ) around the *z* axis is 9.8°. These values are comparable to those estimated from the reported coordinates for $CaMn_{0.5}Nb_{0.5}O_3$ (φ = 13.5°, ψ = 10.3°) and $CaMn_{0.5}Sb_{0.5}O_3$ (φ = 13.8° and ψ = 10.3°).[6]

We have also investigated the structure of the analogous Cu containing oxide $LaCu_{0.5}Rh_{0.5}O_3$, which has not been reported before. Although $LaCuO_3$ can be prepared only at high oxygen pressure,[21] doped samples that also contain Cu^{3+}, such as $LaCu_{0.5}Ni_{0.5}O_3$, can be prepared under milder conditions,[22] albeit in a heterogeneous state. Figure 4 shows the synchrotron X-ray and neutron powder diffraction patterns for $LaCu_{0.5}Rh_{0.5}O_3$ obtained at room temperature. Examination of the synchrotron profile revealed well resolved splitting of the 110 reflection near 2θ = 16.5° indicative of orthorhombic (or lower) symmetry, as well as superlattice reflections associated with both in-phase and out-of-phase tilting of the octahedra. On the basis of previous reports that La_2MgRhO_6 and La_2ZnRhO_6[23] as well as La_2CuIrO_6[24] exhibit cation ordering, a model based on a fully ordered cation distribution in combination with $a^-b^+a^-$ tilting (space group $P2_1/n$) was investigated. Refinement of this model suggested that the monoclinic angle β was very close to 90° and the fit overestimated the intensity of a number of the *R*-point superlattice reflections associated with cation ordering. This problem was addressed by allowing for antisite disorder of the Cu and Rh cations and subsequent refinements suggested a random distribution of these two cations. Accordingly the data were then fitted to a model in *Pbnm* where the Cu and Rh cations are fully disordered. As evident from Figure 4, this leads to an acceptable fit of the synchrotron X-ray diffraction data.

To obtain a more precise description of the *B*−O bond distances the structure of $LaCu_{0.5}Rh_{0.5}O_3$ was refined using powder neutron diffraction data, in the expectation that such data will be more sensitive to displacement of the oxygen atoms. The neutron data are less sensitive than the X-ray data to the possibility of the ordering of the Cu

(20) Chatterji, T.; Ouladdiaf, B.; Mandal, P.; Bandyopadhyay, B.; Ghosh, B. *Phys. Rev. B* **2002**, *66*, 054403.
(21) Demazeau, G.; Parent, C.; Pouchard, M.; Hagenmul, P. *Mater. Res. Bull.* **1972**, *7*, 913–920.
(22) Odier, P.; Municken, M.; Crespin, M.; Dubois, F.; Mouron, P.; Choisnet, J. *J. Mater. Chem.* **2002**, *12*, 1370–1373.
(23) Schinzer, C.; Demazeau, G. *J. Mater. Sci.* **1999**, *34*, 251–256.
(24) Anderson, M. T.; Greenwood, K. B.; Taylor, G. A.; Poeppelmeier, K. R. *Prog. Solid State Chem.* **1993**, *22*, 197–233.

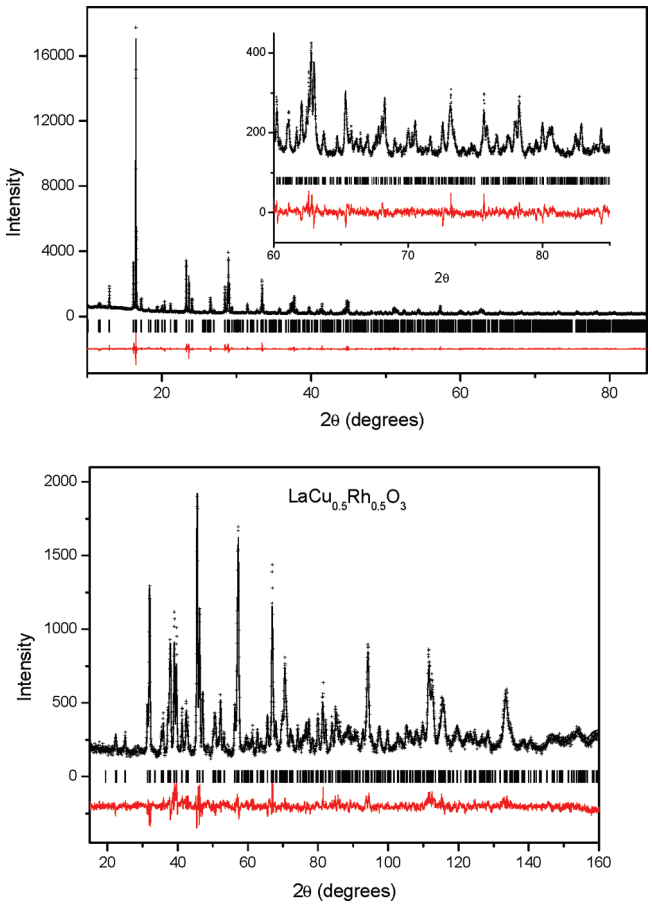

Figure 4. Observed, calculated, and difference synchrotron X-ray (top) and neutron (bottom) diffraction patterns for $LaCu_{0.5}Rh_{0.5}O_3$ refined in *Pbnm*. The inset to the X-ray profile highlights the quality of the data and fit to high angles.

and Rh cations. Refinement of the oxygen occupancies suggests that these are fully occupied. The final results of this refinement are summarized in Table 1. The refined *B*−O distances are 2.023(1), 2.033(3), and 2.073(3) Å, average 2.043 Å, demonstrating the presence of irregular BO_6 octahedra ($\Delta d \approx 1.1 \times 10^{-4}$). The average *B*−O distance in $LaCu_{0.5}Rh_{0.5}O_3$ (2.043 Å) is similar to that reported for $LaRhO_3$ (2.053 Å) although the distortion of BO_6 octahedra is smaller in $LaRhO_3$ ($d \approx 0.25 \times 10^{-4}$).[18] The bond valence sums for Cu in $LaCu_{0.5}Rh_{0.5}O_3$, calculated using the refined *B*-O distances, is 2.61, suggesting partial oxidation of Cu. The calculated value for the Rh, 3.05, is somewhat lower than expected from the XANES measurements and possibly reflects some local disorder of the oxygen anions.

A feature of the neutron profile of $LaCu_{0.5}Rh_{0.5}O_3$ is the diffuse intensity in the form of a modulated background, indicative of short-range correlations in the displacements of some atoms. That this is more evident in the neutron pattern than the X-ray diffraction data suggests that there is some local disorder of the oxygen anions. Such disorder may be induced by short-range ordering of the Rh and Cu cations. A similar effect was observed in the disordered mixed perovskite $CaNb_{0.5}Mn_{0.5}O_3$.[6] The profile for $LaMn_{0.5}Rh_{0.5}O_3$ displayed a more regular background.

It is well-known that large differences in ionic size and oxidation state between the two *B*-site cations are two main factors that favor cation ordering in $AB_{0.5}B'_{0.5}O_3$ perovskites.[24] Because the size difference between Cu^{2+} (ionic radii of 0.73 Å) and Rh^{4+} (0.60 Å) is similar to that between Cu^{3+} (0.54 Å) and Rh^{3+} (0.665 Å),[25] the former pair is more likely to be ordered. Both ordered and disordered arrangements are observed in $AB_{0.5}B'_{0.5}O_3$ perovskites when the difference in the oxidation state between the *B* and *B*′ cations is two. Although rare, disorder can also occur for greater charge differences as exemplified by $Sr_2CuTaO_{5.5}$, which adopts the ideal $Pm\bar{3}m$ perovskite structure with the Cu^{2+} and Ta^{5+} (ionic radii 0.64 Å) cations disordered onto a single site. This symmetry requires that the six *B*−O distances all be equal, that is, the Cu^{2+} cations cannot exhibit a static Jahn−Teller distortion. In this case, it is thought that the presence of a significant level of oxygen vacancies play an important role in the stabilization of the cubic structure.[26,27]

Our structural studies show that the substitution of 50 mol % Cu for Rh in $LaRhO_3$ results in the Cu occupying the same site as the Rh cation, although it induces greater distortion of the BO_6 octahedra that may be a consequence of a JT distortion indicative of a formally Cu^{2+} cation. The CuO_6 octahedra in the cation ordered perovskite Ba_2CuUO_6 shows large tetragonal distortion where the two axial Cu−O(1) bond distances 2.400(2) Å are 0.404 Å longer than the four equatorial Cu−O(2) bond distances 1.996(3) Å.[28] Similar distortions are seen in other ordered perovskites such as Sr_2CuWO_6 and Ba_2CuWO_6.[29] The bond distance anisotropy in $LaCu_{0.5}Rh_{0.5}O_3$ is approximately 10% of this, being about 0.05 Å. There are few well-characterized oxides that contain both Cu and Rh, one example being Sr_3CuRhO_6 that contains an ordered Cu−Rh arrangement[30] in which the Cu atoms are essentially square planar with four short (1.96−2.02 Å) and two long (2.77 Å) distances. The Rh cations are in a slightly distorted octahedral arrangement with an average Rh−O distance of 2.011 Å,[30] which is typical for a Rh^{4+} oxide. There are a number of examples of Cu^{2+} oxides existing in a regular octahedral environment. For example, Köhl and Reinen[31] reported that the Cu−O distances in the CuO_6 octahedron of ordered hexagonal perovskite $Ba_3CuSb_2O_9$ were 2.065 and 2.080 Å, demonstrating the absence of a static Jahn−Teller distortion, although they suggested that a dynamic JT effect may be present.

(25) Shannon, R. D. *Acta Crystallogr., Sect. A* **1976**, *32*, 751–767.
(26) Kato, S.; Ogasawara, M.; Sugai, M.; Nakata, S. *Catal. Surv. Asia* **2004**, *8*, 27–34.
(27) Kato, S.; Sugai, M.; Ohshima, Y.; Takizawa, H.; Endo, T. *Solid State Ionics* **1998**, *108*, 337–341.
(28) Zhou, Q.; Kennedy, B. J. *J. Phys. Chem. Solids* **2007**, *68*, 1643–1647.
(29) Iwanaga, D.; Inaguma, Y.; Itoh, M. *J. Solid State Chem.* **1999**, *147*, 291–295.
(30) Stitzer, K. E.; Henley, W. H.; Claridge, J. B.; zur Loye, H. C.; Layland, R. C. *J. Solid State Chem.* **2002**, *164*, 220–229.
(31) Köhl, P.; Reinen, D. *Z. Anorg. Allg. Chem.* **1977**, *433*, 81–93.

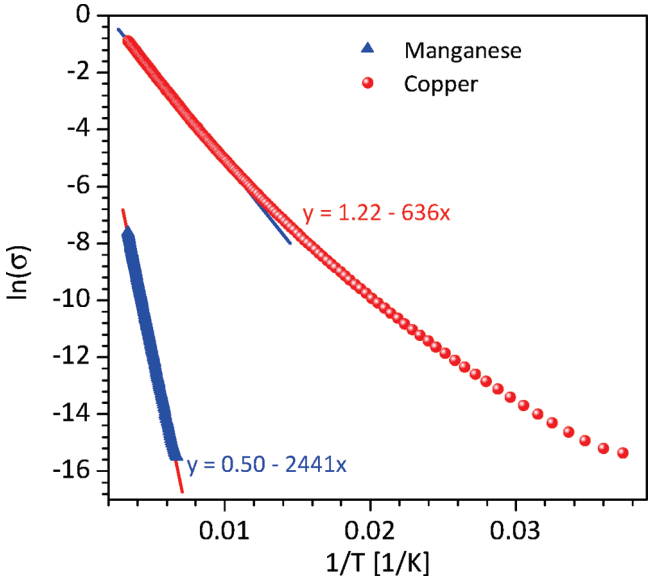

Figure 5. Arrenhius plots of log σ verses inverse temperature for $LaMn_{0.5}Rh_{0.5}O_3$ and $LaCu_{0.5}Rh_{0.5}O_3$. The solid lines are the linear fits to data.

We suggest that the situation in $LaCu_{0.5}Rh_{0.5}O_3$ is similar to that in $CaMn_{0.5}Ru_{0.5}O_3$[32] where an extensive delocalization of charge occurs between the Mn and Ru cations, so that the formal valency of the Cu is close to 2.5, a Jahn−Teller like distortion of the BO_6 octahedra is evident albeit on a much reduced scale compared to a "pure" Mn^{3+} system such as $LaMnO_3$.

The temperature dependence of the resistivity of $LaMn_{0.5}Rh_{0.5}O_3$ and $LaCu_{0.5}Rh_{0.5}O_3$ is plotted in Figure 5 and demonstrates the two oxides are semiconductors in the temperature range studied. In both cases an increase in resistivity with decreasing temperature is observed, with the resistance exceeding the maximum value that could be measured ($R > 1 \times 10^7$ Ω) near 150 K for $LaMn_{0.5}Rh_{0.5}O_3$ and 25 K for $LaCu_{0.5}Rh_{0.5}O_3$. An Arrenhius plot of log σ verses inverse temperature for $LaMn_{0.5}Rh_{0.5}O_3$ reveals linear dependence indicative of a semiconductor with a low activation energy of 0.21 eV. The conductivity of $LaCu_{0.5}Rh_{0.5}O_3$ was noticeably higher than that of the analogous Mn oxide, suggesting electron delocalization between the Cu and Rh cations. The Arrenhius plot gave a lower activation energy, 0.055 eV, for this complex. This is consistent with the observed XANES results that suggest mixed valence in $LaCu_{0.5}Rh_{0.5}O_3$.

The magnetic properties of both compounds were also examined. Measurements of the magnetization of $LaMn_{0.5}Rh_{0.5}O_3$ as a function of applied field and temperature show this to be ferromagnetic with a Curie Temperature T_c of 65(1) K in reasonable agreement with 72(1) K reported by Schinzer.[7] Given the XANES measurements demonstrate the presence of diamagnetic

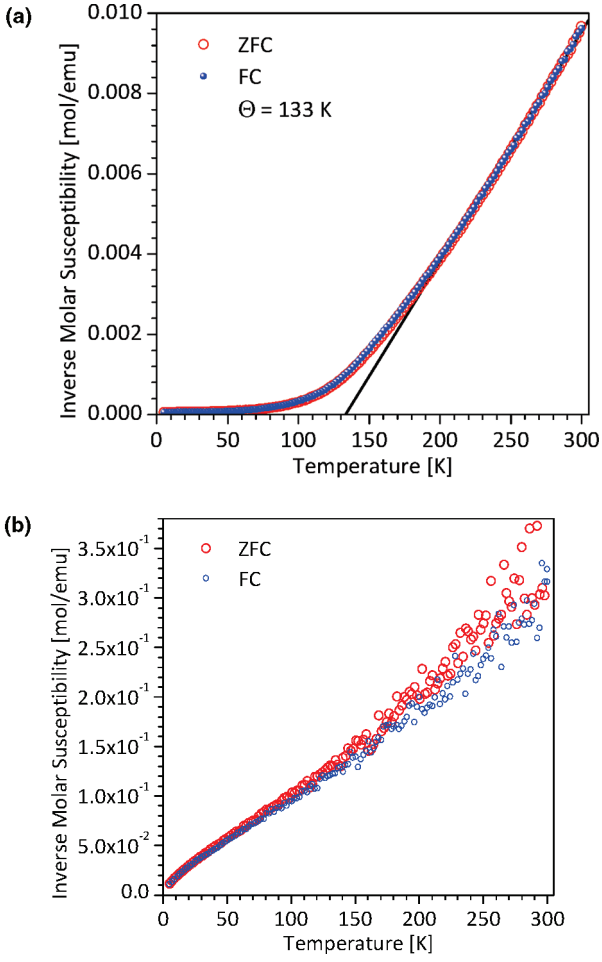

Figure 6. Inverse molar susceptibility for (a) $LaMn_{0.5}Rh_{0.5}O_3$ and (b) $LaCu_{0.5}Rh_{0.5}O_3$. The line in $LaMn_{0.5}Rh_{0.5}O_3$ represents the best fit to the Curie−Weiss law in the paramagnetic region.

Rh^{3+}, and the diffraction shows disorder of the Mn^{3+} and Rh^{3+} cations the ferromagnetism presumably arises through vibronic superexchange between Mn^{3+}−O−Mn^{3+} interactions. $LaCu_{0.5}Rh_{0.5}O_3$ is only very weakly paramagnetic, Figure 6, and magnetic hysteresis loops show no evidence for any long-range magnetic interactions. Although the details of the magnetic structure of $LaMn_{0.5}Rh_{0.5}O_3$ are still to be fully resolved, the present work serves as a cautionary tale in assigning valence states in strongly coupled systems on magnetic data alone.

Conclusions

In summary, it has been established using XANES measurements that both the Mn and Rh in $LaMn_{0.5}Rh_{0.5}O_3$ are trivalent. The structure has been refined from neutron diffraction data and the absence of an appreciable JT distortion of the BO_6 octahedra is a consequence of the disorder of the Mn^{3+} and Rh^{3+} cations onto the same site and large magnitude of the octahedral tilting. XANES measurements also show the Rh in $LaCu_{0.5}Rh_{0.5}O_3$ with a valence state of around +3.5. The extensive delocalization of charge occurring between the Cu and Rh cations increases the

(32) Zhou, Q.; Kennedy, B. J.; Zhang, Z.; Jang, L.-Y.; Aitken, J. B. Chem. Mater. **2009**.

formal valency of the Cu to close to 2.5, which reduces the impact of a Jahn−Teller like distortion of the BO_6 octahedra. The distortion of the octahedra in $LaCu_{0.5}Rh_{0.5}O_3$ ($\Delta d \approx 1.1 \times 10^{-4}$) is slightly smaller than that seen in $LaMn_{0.5}Rh_{0.5}O_3$ ($\Delta d \approx 1.9 \times 10^{-4}$), but much smaller than that in the "pure" Mn^{3+} system $LaMnO_3$ ($\Delta d \approx 33.1 \times 10^{-4}$).

Acknowledgment. This work has been partially supported by the Australian Research Council. The synchrotron studies were supported by the Australian Synchrotron Research Program under the Major National Research Facilities Program. The synchrotron X-ray diffraction experiments at the ANBF were performed with the help of Dr. James Hester.